Two-day Wave Observations of UARS-MLS Mesospheric Water Vapor and Temperature

Varavut Limpasuvan[1] and Dong L. Wu[2]

[1] Department of Chemistry and Physics, Coastal Carolina University, Conway, South Carolina.

[2] Jet Propulsion Laboratory, California Institute of Technology, Pasadena, California

Short title: TWO-DAY WAVE IN THE MESOSPHERE

In preparation for submission to J.G.R.

Abstract

The two-day wave disturbance is observed in the mesospheric temperature and water vapor based on new version data from the Upper Atmosphere Research Satellite Microwave Limb Sounder. Using two data segments during the Austral summers (January-February of 1992 and 1993) and the asynoptic mapping method, the strong wave signal is identified as zonal wavenumber 3 and westward period of about 2.1 days. The wave amplitudes are located near the core of the summer easterly jet with strongest wave amplitudes (as large as 11 Kelvins and 0.35 part per million by volume) near the mesopause. The temperature and water vapor wave strengths are highly correlated in time but their peaks are almost longitudinally out-of-phase. Poleward heat flux associated with upward wave energy propagation in the southern hemisphere points to baroclinic instability as the cause for the wave appearance. Growing wave signature in water vapor is observed in regions of strong meridional gradient of water vapor. Near the mesopause, wave breaking is suggested as moist polar air is displaced into the much drier subtropics and wave amplitude decays.

1. Introduction

The two-day wave is a recurring phenomenon, readily observed just after the solstice. The wave can be found in the upper stratosphere up through the thermosphere and typically persists for 15-30 days. As a zonal wavenumber 3 disturbance that propagates westward with a period of about 2 days, the wave amplitude resides in close proximity to the summer easterly jet core where the vertical and meridional wind shears are very strong. As such, its existence has been attributed to the instability of the summer easterly jet [e.g. *Plumb*, 1983; *Pfister*, 1985; *Randel*, 1994]. On the other hand, because of its recurring nature and lack of known forcing mechanisms, the wave appearance has also been explained as the amplification of a global normal resonance mode [*Salby*, 1981].

Observations by single station measurements [e.g. *Harris*, 1994; *Palo et al.*, 1997; *Herman et al.*, 1999; *Fritts et al.*, 1999] and various satellite instruments [e.g. *Burks and Leovy*, 1986; *Wu et. al.*, 1993 and 1996; *Shepherd et al.*, 1999; *Lieberman*, 1999; *Azeem et al.*, 2001] reveal the two-day wave to be particularly strong in the mesosphere despite the presence of strong thermal damping (less than 0.2 $days^{-1}$) and mechanical damping (mainly gravity wave drag) at these altitudes [e.g. *Garcia*, 1989]. At low summer latitudes, the maximum meridional and zonal wind amplitudes are ~60 m/s and ~20 m/s, respectively. At middle summer latitude, the temperature wave amplitude can be greater than 5 K.

Because of these large amplitudes, the two-day wave disturbance may also be present in chemical species like ozone and water vapor. Recently, *Azeem et al.* [2001] identified the wave signature in ozone and suggested it to be photochemically driven by the corresponding temperature perturbations through changes in reaction rates. However,

global observations of the two-day wave disturbance in mesospheric water vapor do not exist. The lone previous observations of the two-day wave in water vapor was in the upper stratosphere by *Limpasuvan and Leovy* [1995]. In general, mesospheric water vapor has garnered much interests. Because it has strong vertical gradient in the upper mesosphere as a result of diminishing photochemical lifetime with altitudes, water vapor serves as a great indicator for atmospheric transport [e.g. *Nedoluha et al.*, 1996; *Pumphrey and Harwood*, 1997]. Moreover, its presence is intimately linked to noctilucent clouds that appear over the extremely cold polar summer mesopause [e.g. *Garcia*, 1989 and reference therein]. These clouds have been linked to increasing greenhouse gases and global change [e.g. *Olivero and Thomas*, 2001].

In this paper, we present observations of the two-day wave disturbance in mesospheric water vapor and temperature. Such a study may shed additional light on the structure and mechanism of the two-day wave. To our knowledge, this study is the first to elucidate global two-day wave signature in water vapor at the mesospheric level. In our results, the water vapor two-day wave signature dominates the total field (particularly where the meridional gradient of water is strong) and is consistent with baroclinic instability of the easterly jet. Additionally, mixing of water vapor field by the two-day wave is suggested in the low summer latitudes through wave breaking processes.

2. Data and Analysis

We use the newly available data of the Microwave Limb Sounder (MLS) [*Barath et al.*, 1993], an instrument on the Upper Atmosphere Research Satellite (UARS) [*Reber et al.*, 1993]. Launched in late 1991, the UARS is a sun-synchronous, polar orbiting satellite that completes ~14 orbits in a day. The water vapor mixing ratio is retrieved from the

180-GHz H_2O line and extends approximately from 15 km to 90 km. As discussed in *Livesey et al.* [2002], the version (v5) data represents significant improvement and advancement in retrieval algorithm and processing software over previous MLS data versions. Subsequently, the v5 data has improved data quality and vertical resolution, particularly in the mesosphere. The temperature data is retrieved from O_2 63-GHz emission with a separate algorithm (accounting for the geomagnetic Zeeman effect) and covers altitudes of 20-90 km [*Wu et al.*, 2002]. This retrieval uses a single temperature profile (an annual mean) as the first guess and linearization point.

For analysis, we begin with the unbinned along-track vertical profiles (Level 3AT) of MLS mesospheric temperature and water vapor (H_2O) data. The vertical resolution of the H_2O profiles is ~3 km in the stratosphere and ~5 km in the mesosphere. The vertical resolution for temperature is ~8 km in the stratosphere and ~14 km in the mesosphere. We then compute the spectra from the temperature and water vapor data at each level using the asynoptic mapping method of *Salby* [1982ab] to resolve signals with periods greater than 1 day. Application of this method to earlier version of MLS data is discussed in *Elson and Froidevaux* [1993], *Canziani et al.* [1994], *Limpasuvan and Leovy* [1995], and *Lieberman* [1999].

While the MLS data set is available from September 1991 to 1999, measurements after December 1994 are generally sparse, with no consecutive observations greater than 8 days [cf. appendix of *Livesey et al.*, 2002]. As the asynoptic method is grounded on Fourier transform technique, relatively long time series is necessary for acceptable spectral resolution and many cycles of the two-day wave. A time series of less than 8 days approximately contains only 112 measurements (i.e. 8 days at ~14 orbits a day) at a

given latitude. After tapering 10% of the series at each end, the number of measurements is effectively reduced to ~90. To maintain relatively high spectral resolution, we avoid data after 1994. Furthermore, the UARS performs a yaw-around maneuver every 30-40 days (a "yaw period") to keep some instruments from pointing at the sun. The data spatial coverage is thus not truly global but rather extends from 80^o latitude in one hemisphere to about 30^o latitude of the other.

As the two-day temperature wave (of zonal wavenumber 3) is previously observed mainly in the southern hemisphere during Austral summers, two relatively long data series are analyzed: (1) January 15 - February 14, 1992, and (2) January 5-February 8, 1993. These data segments represent two yaw periods. The corresponding latitudinal coverage is between 80^oS and 30^oN. In practice, spatial coverage is limited to 28^o and 68^o. Data poleward of 68^o is avoided because profiles taken during northward (or ascending) and southward (or descending) satellite path become less distinct, causing numerical problems in the asynoptic mapping [*Lait and Stanford*, 1988].

In the literature, the two-day wave is sometimes defined to include a wavenumber 4 disturbance with period of ~1.8 days [*Wu et al.*, 1996; *Lieberman*, 1999; *Limpasuvan et al.*, 2000]. During the Boreal summers (June-August) after the solstice, the wavenumber 4 generally dominates its wavenumber 3 counterpart and appears to be purely an instability mode. In the present paper, focus is placed strictly on the wavenumber 3 two-day wave, which is the dominant spectral signature for the chosen data segments (see below).

3. Results

A. Spectral Signature and Wave Structure

Fig. 1 shows the wavenumber-frequency spectra for water vapor and temperature in the mesosphere during the analyzed segments. The spectra are averaged between 70^{o}S and 18^{o}S and between 0.10 and 0.0046 hPa (65-86 km). Clearly, the dominant signature in both species is a westward-propagating, zonal wavenumber 3 disturbance with central period of ~2.1 days (about 0.48 cycles per day, cpd). The signal is consistent during each observed segments in the summer mesosphere. In this paper, we will refer to "two-day wave" as being associated with the spectral peak between 0.35 and 0.60 cpd (as noted in Fig. 1).

Fig. 2 (top two rows) shows the amplitude distribution of the two-day wave in water vapor and temperature. Illustrated as filled contours, the wave amplitude is computed as the square root of the wavenumber 3 power spectra integrated over 1.67-2.86 days (0.35-0.60 cpd) at each level. The amplitude is plotted where the coherence squared with respect to the reference point is significant at the 95% level or greater (for approximately 5 degrees of freedom). This reference point is at the position where the amplitude is largest in the summer mesosphere (i.e. around 80 km and 40^{o}S).

Consistent with the spectral information, the temperature amplitude structure is mainly confined in the summer hemisphere and is remarkably similar in both years. Strongest magnitude appears around the mid-latitude region of the upper mesopause (~80 km). Throughout much of the mesosphere down to the stratopause, the wave amplitude structure tilts equatorward. A secondary maxima appears around 65 km. Near the stratopause (~50 km), the two-day wave amplitude is mostly in the subtropical region. These structures in the lower mesosphere and upper stratosphere concur with observations of previous versions of the MLS temperature data [*Limpasuvan and Leovy*

1995; *Wu et al.*, 1996; and *Limpasuvan et al.*, 2000]. Finally, we note that the strength of the two-day wave amplitude is slightly stronger during 1993.

The two-day wave in the water vapor data has a similar amplitude distribution as the temperature. A relatively strong peak appears near the mesopause level, but is more equatorward with respect to the temperature peak near the same level. As with the temperature data, the amplitude peak is stronger during the 1993 observations. Wave signature in the lower mesosphere is also evident in water vapor and is slightly equatorward of the peak aloft. During the 1992 observations the peak in water vapor amplitude near the 50 km level has comparable strength to the amplitude near the mesopause. Such strong two-day wave signature in water vapor near the stratopause was noted by *Limpasuvan and Leovy* [1995] for the same year.

Also shown in Fig.2 are distributions of MLS gravity wave variances observed around the same time interval as the two-day wave. These variances measure gravity wave activities at short horizontal (~100km) but long vertical (>10km) scales, providing additional information on atmospheric variability and instability. Details of MLS gravity wave retrievals are discussed in *Wu and Waters* [1996]. During the periods of interest, we note that the gravity wave variance increases along the easterly jet core, similar to the variation of the two-day wave amplitudes, showing the poleward tilt as height increases. Again consistent with the two-day wave, the gravity wave variance is generally larger in 1993 than in 1992. Further discussions on gravity wave are provided in Section 4.

The meridional cross-section description is essentially only a time average representation of the wave structure during each of the chosen data segments. In general, the wave evolution appears to be episodic (i.e. pulse-like) and subsequently its structure

can be variable (cf. Figs. 4-5). Examining the structure over the entire yaw periods results in a weak (or "smeared") representation of the wave structure. In addition, given the wave's episodic nature, a clean meridional cross-section representation of the wave phase structure over the 20-30 day interval is difficult to obtain [cf. *Burks and Leovy*, 1986; *Limpasuvan and Leovy*, 1995]. Therefore, to elucidate the wave phase structure we can simply examine the perturbation field associated with the two-day wave in height-longitude sections and longitude-latitude sections during the time of strongest wave activity. Here, the perturbation is obtained by integrating the wavenumber 3 spectral over the frequency range illustrated in Fig. 1.

Fig. 3 demonstrates the wave phase for January 26, 1992. Nearly identical phase structure is observed in the 1993 observation (see also Fig. 8). The phase of the two-day wave generally tilts westward with height above 60 km; this westward tilt is more obvious in the temperature results. Such westward vertical tilt is indicative of upward energy propagation for planetary-scale waves as determined by their dispersion relation if the zonal wavenumber is taken to be positive [*Andrews et al.*, 1987]. In the meridional direction, the wave phase tilts equatorward in the northward direction throughout the summer hemisphere. From the same dispersion relation, the wave energy is inferred to be directed toward the equator.

B. Time Evolution

The episodic nature of the two-day wave in the mesosphere is shown in Fig. 4. The two-day wave amplitude is plotted as a function of latitude and time at 0.01 hPa (about 80 km). The wave amplitude can reach as high as 0.35 ppmv for water vapor and 11 K for the temperature. Remarkably, the amplitude variation of the water vapor wave nearly

parallels that of the temperature wave. In particular, during Jan.-Feb. 1992, near-concurrent wave peaks appear around Jan. 20, Jan. 27, and Feb. 6. Consistent with the amplitude structure (cf. Fig. 2), the water vapor amplitude is slightly equatorward of the temperature amplitude.

To highlight the relationship between water vapor and temperature waves, we compute the temporal correlation of their wave amplitudes at each height and latitude (see Fig. 5). Correlation greater than 0.5 appears near the mid-latitude, mesopause region and near subtropical, middle mesosphere (near 60 km). Around 80 km and 40^{o}S, the correlation value exceeds 0.90 for both years. High correlation value means that the strength of temperature and water vapor wave perturbation tends to peak at the same time as noted in Fig. 4. However, such temporal correlation value does not reveal the relative phase of the wave amplitude.

The relative phase difference between the temperature and water vapor wave is given in the bottom two rows of Fig. 5. The phase difference is related to the difference in the longitudinal positions of the wave perturbation extrema. For zonal wavenumber 3 disturbance (such as the two-day wave), a 60^{o} displacement in longitudes between the wave extrema corresponds to an out-of-phase (or 180^{o} phase difference). Near the mesopause (0.01 hPa), the observed phase difference tends to be 180^{o} during the entire observed time of each year. This out-of-phase relationship is apparent for all latitudes between 30^{o}-46^{o}S. In fact, this phase difference is apparent in Fig. 3 as the shaded regions (negative perturbations) tend to overlap the unshaded regions (positive perturbations). At lower altitude (e.g. 60 hPa) where the temporal correlation values are generally smaller, the phase difference are more variable and not as focused at 180^{o} (see bottom row of Fig.

5).

4. Discussion

A. Structure and instability

Overall, the wave amplitude resides near the top side of the summer easterly jet core where the zonal wind can be in excess of 70 m/s on a day-to-day basis. To get a sense of the corresponding wind structure, we superimpose onto Fig. 2 the CIRA climatological zonal wind [*Fleming et al*, 1990] averaged for January and February (none-filled contours). Clearly, the wave amplitudes tend to collocate with regions of strong vertical and meridional wind shear that are typically just equatorward or above the easterly jet core. Strongest wave peak near the mesopause coincides with the levels where the easterly jet closes off (about 80-90 km).

As mentioned in the Introduction, the described strong wind shears have led previous authors to link the two-day wave to barotropic/baroclinic instability [e.g. more recently by *Lieberman*, 1999; *Fritts et al.*, 1999]. These studies show that the zonal mean wind structure exhibits regions of reversed potential vorticity gradient near the summer easterly jet core. Theoretically, *Plumb* [1983] and *Pfister* [1985] demonstrated that the fastest growing unstable mode with a westward propagating period of near two days is possible for a reasonably realistic easterly jet structure.

Throughout the mesosphere, gravity wave breaking provides the strong westward forcing to decelerate the easterly jets and likely accounts for the wind shears. Indeed, the westward acceleration by gravity wave forcing helps cap the summer easterly jets near the mesopause and drives the summer to winter pole circulation at those levels [*Leovy*, 1964; *Andrews et al*., 1987]. The connection of gravity wave in the mesosphere with the

two-day wave was demonstrated in the modeling work of *Norton and Thuburn* [1996; 1997]. In those studies, the simulated two-day wave amplitude structure, the region of westward forcing by gravity waves, and areas of reversed potential vorticity gradient collocate along the equatorward flank of the easterly jet with the upward tilt toward the summer pole. When the wind shear was weakened by introducing weak gravity wave drag, the two-day wave was noticeably absent. Remarkably, the double peak wave structure of the temperature field observed here (c.f. Fig. 2) is very similar to the modeled results of *Norton and Thuburn* in both its latitude and altitude location.

Gravity waves may play two roles in the two-day wave generation. First, strong wind shears stresses the importance of gravity waves in accelerating the mean wind and setting up regions of instability for the two-day wave to proliferate. Second, by interacting with the background, gravity waves may directly provide a longtitudinally-varying drag in the upper mesosphere that could serve as the seed of instabiliy modes. The MLS variance maps show the gravity wave activities are highly varied in the Southern Hemisphere during December-Feburary due to convective and topography sources in the lower atmosphere.

The phase structure of the two-day wave observed in this study suggests ties to instability. As illustrated in Fig. 3, the phase tilt with height indicates upward energy propagation of the wave based on the dispersion relationship of planetary-scale waves. The upward energy propagation is consistently with the southern summer mesosphere observations of *Lieberman* [1999] and *Fritts et al.* [1999] who analyzed the High Resolution Doppler Image (HRDI) on UARS and single-station radar winds and temperature during 1992-1994. In these studies, the 2-day temperature perturbations are

clearly *out-of-phase* with the meridional wind; therefore, the heat flux ($\overline{v'T'}$) is negative. [Here, the overbar denotes zonal average, and the prime indicates departure from the zonal average]. The path of wave energy propagation can be related to the Eliassen-Palm (EP) flux (***F***) whose vertical component is governed by heat flux [*Andrews et al.*, 1987]:

$$F_z \approx f_o \rho_o \overline{v'T'} \qquad (1)$$

where f_o is the Coriolis parameter and ρ_o is the background density. Given the two-day temperature perturbation in the southern hemisphere during January-February, negative heat flux implies upward energy propagation. These studies also demonstrated the EP flux vectors to emanate from regions of negative potential vorticity gradient, suggesting an *in situ* wave source from the wave's critical line. Similar two-day wave energy radiation from an unstable region was modeled by *Limpasuvan et al.* [2000].

B. Mean Tracer Gradient and Observed Amplitude

Several daily cross-sections of the summer hemisphere H_2O distribution are shown in Fig. 6 around the time of strong two-day wave activity. Water vapor enters into the middle atmosphere typically through the cold tropical tropopause. In the stratosphere, water vapor is generated *in situ* by the oxidation of methane. Near the stratopause, nearly all of methane is depleted and converted to water vapor. Above the stratopause, the water vapor concentration begins to diminish because of photodissociation due to absorption of solar radiation at wavelengths near Lyman α [e.g. *Nedoluha et al.*, 1996]. The lifetime of water molecules is on the order of several months near the stratopause; however, its lifetime at 80 km and above is only a few days [e.g. *Garcia*, 1989; *Pumphrey and Harwood*, 1997]. Generally, above 60 km, the distribution of water vapor is a result of

the competition between transport (advective and diffusive) and photodisssociation. The vertical variation in lifetime accounts for strong vertical gradient in the water vapor field, particularly near the upper mesosphere.

The observed latitudinal variation of water is however governed largely by vertical, advective transport. Below 50 km, the H_2O distribution has an inverted Gaussian shape with minimum mixing ratio near the equator and relatively large concentration (greater than 7.0 ppmv) in the high summer latitudes. Such equatorial bulge in the distribution is consistent with a rising motion in the tropics that keeps the region relatively dry despite the present of water vapor source due to methane oxidation throughout the stratosphere. Subsequently, negative meridional gradient (decreasing concentration with latitude) is evident below 50 km. A relatively stronger negative meridional gradient in H_2O exists in the mid-latitude, upper mesosphere region (~80 km). This gradient is associated with an overturning mean meridional circulation driven primarily by gravity waves [e.g. *Garcia and Solomon*, 1985] in the mesosphere: with upwelling at the summer pole, meridional movement from the summer pole to winter pole, then downwelling at the winter pole. We note that the strong tracer gradient near 40^oS between 70-90 km is probably an artifact of the MLS water data due to the *a priori* used for retrieving water. This aberration is obvious in all zonal mean cross-sections.

During 1992, the meridional tracer gradient in the low summer latitudes (20^oS-40^oS) near the stratopause (40-50 km) is noticeably stronger than 1993. This stronger meridional gradient is evident by the presence of the 4.8-5.2 ppmv band at higher altitude (around 1 hPa) during 1992. The stronger meridional gradient of the water vapor in the subtropics during 1992 is associated with stronger upwelling in the equatorial upper

stratosphere. This strong upwelling may be linked to the strong polar warming episodes during the 1992 winter [eg. *Farman et al*., 1994]. In the H_2O wave structure shown in Fig. 2, the relatively strong amplitude in upper stratospheric region (1 hPa or about 50 km) during 1992 can perhaps be related to the difference in the described tracer gradient.

The importance of background tracer gradient can be seen by considering the linearized continuity equation for a conservative tracer (χ) in Cartesian coordinate (x, y, z) as given in *Andrews et al.* [1987]:

$$(\frac{\partial}{\partial t} + \bar{u}\frac{\partial}{\partial x})\chi' + v'\bar{\chi}_y + w'\bar{\chi}_z = 0 \qquad (2)$$

Here, the subscript indicates partial derivative. Neglecting advection by vertical wind perturbation (w'), we can multiply the above equation by (χ'), and take the zonally average to get:

$$\frac{\partial}{\partial t}\overline{\chi'^2} = -2(\overline{v'\chi'})(\bar{\chi}_y) \qquad (3)$$

This equation states the dependence of the local time change of the tracer variance on the tracer meridional flux ($\overline{v'\chi'}$) and the background tracer meridional gradient ($\bar{\chi}_y$).

For water vapor, equation 3 may be directly applicable in the lower mesosphere and upper stratosphere where the chemical life time remains relatively long. Water vapor in that altitude range can be considered as a near-conservative tracer. However, the photochemical timescale of water becomes relatively small (about a few days) in the upper mesosphere, implying that water vapor may not be truly conservative at these altitudes. Nonetheless, as presented below, the above equation can quantitatively explain the H_2O two-day oscillations near the mesopause.

For a growing wave perturbation, the right hand side of equation 3 must be positive. Since the (background) meridional gradient of water vapor is always negative (cf. Fig. 6), the associated wave flux must be down the mean tracer gradient resulting in equatorward or positive tracer flux in the summer hemisphere. This is shown schematically in Fig. 7 for water vapor which has a minimum mixing ratio near the equator (cf. Fig. 6).

Such positive tracer meridional flux is consistent with the observed out-of-phase relationship between water vapor and temperature near the mesopause (cf. middle row of Fig. 5). Recall that *Lieberman* [1999] and *Fritts et al*. [1999] found the temperature and meridional wind perturbations to be out-of-phase. This then implies that the meridional wind and water vapor perturbations must be in phase and ($\overline{v'\chi'}$) must be positive or equatorward.

Equation 3 also suggests that, to observe strong wave amplitude in the tracer, relatively strong background meridional gradient of the tracer must be present. During 1992, stronger H_2O wave amplitude is observed near 50 km because of a more pronounced background tracer gradient despite comparable two-day wave signature in the 1993 temperature field. In association with the strong meridional gradient in the upper mesosphere, we also see a well-defined structure of the two-day wave in the water vapor field concentration in the polar region. For the same reasoning, we may attribute the diminished amplitude in the water vapor wave signature around the region of 55-65 km to the weak gradient in the H_2O field although the two-day temperature wave is quite strong.

C. Total Water Vapor Field and Possible Wave breaking

Fig. 8a and Fig. 8b show the 1993 twice-daily maps of total water vapor at 0.01 hPa (~80 km) and 0.0046 hPa (~86 km), respectively, when the two-day wave is present (cf. Fig. 4). Around 40^{o}-60^{o}S where the meridional tracer gradient is pronounced (cf. Fig. 6), the two-day wave disturbance appears as zonal wavenumber 3 undulations in the isopleths that tilt equatorward to the north (consistent with Fig. 3). Rearrangement of relatively moist (darker) and dry (lighter) air also occurs near 20^{o}S as patches of moist (dry) air are observed equatorward (poleward) of 20^{o}S. These latter features and the isopleth undulations are quite deep, appearing at both presented levels

Based on its large amplitudes, the two-day wave may break in the upper summer mesosphere in a manner similar to planetary waves in the winter hemisphere [*Plumb et al.*,1987; *Limpasuvan and Leovy*, 1995; and *Orsolini et. al.*, 1997]. As noted by *Plumb et al.* [1987], given the large meridional displacement of the two-day wave coupled with the possibility of wave breaking, longer–lived constituents (lifetimes greater than 0.5 days) might exhibit a dramatic response in the mesosphere. Our observations of these water vapor maps suggest that wave breaking may indeed be occuring near the mesopause. The wave breaking appears to be related to the decay process of the two-day wave and the pulsing nature of the two-day wave observed in Fig.4

A dramatic episode occurs around Jan. 21, 1993 when the wave amplitude is very strong. A moist tongue extends from 270^{o}E, 40^{o}S well into 90^{o}E, EQ. At the same time relative dry air on the westward side of the moist tongue protrudes into the summer mid-latitude. After Jan.21 when breaking had occurred, we note several isolated dark and light "blobs" in the subtropics and diminished wavenumber 3 undulation near 40^{o}S. After Jan.

23, the wavenumber 3 undulation again becomes pronounced and amplify. This continue growth culminates into what appears to be another breaking feature around 90^{o}E around Jan. 25. We note that these breaking episodes near location of strong gradient is reminiscent of the tropical "surf zone" in the winter stratosphere [e.g. *Polvani et al.*, 1995].

6. Summary

The two-day wave disturbance is identified throughout the mesosphere using the temperature and water vapor measurements from the UARS MLS during two Austral Summers (January-February of 1992 and 1993). The spectral signature is in agreement with previous observations at lower altitudes, namely of zonal wavenumber 3 and a period of ~2 days. The disturbance is episodic during the observation periods of interest.

The wave amplitudes are located near the core of the summer easterly jet with strongest wave amplitudes (about 7 Kelvins and 0.22 part per million by volume) near the mesopause where the easterly jet closes off. In these regions, gravity wave forcing can account for the strong vertical and meridional shear in the jet and may serve as a seed of instability.

The wave perturbation strength is highly correlated in time. This coherence extends throughout much of the mesosphere and from the middle to lower latitudes. However, the perturbation amplitude tends to be nearly out-of-phase longitudinally. Such phase displacement is more robust in the upper mesosphere but less clearly defined in the lower mesosphere.

The wave structure suggests instability as the cause for the wave appearance. Previous studies of the two-day wave during the same time period generally find an out-

of-phase relationship between temperature perturbation and meridional wind perturbation, as expected for poleward heat flux or upward energy propagation. The observed phase of the wave tilts westward with height which is in agreement with upward propagating planetary waves.

Despite relatively short photochemical lifetime in the upper mesosphere, the two-day wave presence in water vapor is consistently found in regions of strong meridional gradient. In 1992, when the H_2O meridional gradient is large in the upper stratosphere (apparently due to stronger equatorial upwelling during Jan.-Feb.), a more pronounced two-day wave signature is detected in water vapor. Where the background tracer field is more or less homogeneous, the wave disturbance is not readily observable in water vapor even when a strong temperature ampltiude is evident.

The two-day wave signature readily appears in the twice-daily maps of total water vapor as zonal wavenumber 3 undulations of the isopleths. Near the mesopause, as the perturbations fully mature, features reminiscent to wave breaking are evident as overturning of extended tongue of moist and dry air. The breaking process subsequently leads to isolated patches of dry and moist air in the summer subtropics and diminished undulation of the water isopleths.

7. Acknowledgment

This study was supported initially in part by the *South Carolina NASA Space Grant Consortium* and was carried out when VL was a *NASA Summer Faculty Fellowship* at Jet Propulsion Laboratory (JPL). We are especially grateful to Dr. Joe W. Waters for hosting VL and Ms. Linda Rodgers for coordinating this Fellowship program. We are also

thankful the assistance of Drs. Robert P. Thurstans, Jonathan H. Jiang, Yibo Jiang, and Paul Wagner at JPL.

8. References

Andrews, D. G, Holton, J. R., and Leovy, C. B., 1987: Middle Atmosphere Dynamics, Academic Press, 489 pp.

Azeem, S. M. I., S. E. Palo, D. L. Wu, and L. Froidevaux, 2001: Observations of the 2-day wave in the UARS MLS temperature and ozone measurements, Geophys. Res. Lett., 28, 3147-3150.

Barath, F. T. and Coauthors, 1993; The *Upper Atmosphere Research Satellite* Microwave Limb Sounder instrument, *J. Geophys. Res.*, **98**, 10751-10762.

Burks, D. and C. B. Leovy, 1986: Planetary waves near the mesospheric easterly jet, *Geophys. Res. Lett.*, **13**, 193- 196.

Canziani, P. O., J. R. Holton, E. Fishbein, L. Froidevaux, and J. W. Waters, 1994: Equatorial Kelvin waves: A UARS MLS view, *J. Atmos. Sci.*, **51**, 3053-3076.

Elson, L. S. and L. Froidevaux, 1993: Use of fourier transforms for asynoptic mapping: application to the Upper Atmosphere Research Satellite Microwave Limb Sounder, *J. Geophys. Res.*, **98**, 23039-23049.

Farman, J. C., A. O'Neill, and R. Swinbank, 1994: The dynamics of the arctic polar vortex during the EASOE campaign, *Geophys. Res. Lett*., **21**, 1195-1198.

Fleming, E. S., et al., 1990: Zonal mean temperature, pressure, zonal wind, and geopotential height as function of latitude, *Adv. Space Res.*, **10**, 11-59.

Fritts, D. C. J. R. Isler, R. S. Lieberman, M. D. Burrage, D. R. Marsh, T. Nakamura, T. Tsuda, R. A. Vincent, I. M. Reid, 1999: Two-day wave structure and mean flow

interactions observed by radar and High Resolution Doppler Imager, *J. Geophys. Res.*, **104**, 3953-3969.

Garcia, R. R. and S. Solomon, 1985: The effects of breaking gravity waves on the dynamics and chemical composition of the mesosphere and lower thermosphere, *J. Geophys. Res.*, **90**, 3850-3868.

Garcia, R. R., 1989: Dynamics, radiation, and photochemistry in the mesosphere: implications for the formation of noctilucent clouds, *J. Geophys. Res.*, **94**, 14605-14615.

Harris, T. J., 1994: A long-term study of the quasi-two-day wave in the middle atmosphere, *J. Atmos. Terr. Phys.*, **56**, 569-579.

Herman, R. L., W. A. Robinson, and S. J. Franke, 1999: Observational evidence of quasi two-day wave interaction using MF radar, *Geophys. Res. Lett.*, **26**, 1141-1144.

Jiang, J. H. and D. L. Wu, 2001: UARS MLS observations of gravity waves associated with the Arctic winter stratospheric vortex, *Geophys. Res. Lett.*, **28**, 527-530.

Jiang, Y., 2002: EOS MLS Level 3 Algorithm Theoretical Basis, JPL technical report D-18911.

Lait, L. R. and J. L. Stanford, 1988: Applications of asynoptic space-time Fourier transform methods to scanning satellite measurements, *J. Atmos. Sci.*, **45**, 3784-3799.

Livesey, N. J., W. G. Read, L. Froidevaux, J. W. Waters, H. C. Pumphrey, D. K. Wu, M. L. Santee, Z. Shippony, and R. F. Jarnot, 2002: The UARS Microwave Limb Sounder version 5 dataset: theory, characterization and validation, *J. Geophys. Res*., in review.

Leovy, C. B., 1964; Simple models of thermally driven mesosphere circulation, *J. Atmos. Sci*., **21**, 327-341.

Lieberman, R.S., 1999: Eliassen-Palm fluxes of the 2-day wave, *J. Atmos. Sci*., **56**, 2846-2861.

Limpasuvan, V. and C. B. Leovy, 1995: Observations of the two-day wave near the southern summer stratopause, *Geophys. Res. Lett.*, **22**, 2385-2388.

Limpasuvan, V., C. B. Leovy, and Y. J. Orsolini, 2000: Observed temperature two-day wave and its relatives near the stratopause, *J. Atmos. Sci.*, **57**, 1689-1701.

Limpasuvan, V., C. B. Leovy, Y.J. Orsolini, and B. A. Boville, 2000: A numerical simulation of the two-day wave near the stratopause, *J. Atmos. Sci.*, **57**, 1702-1717.

McIntyre, M. E., 1989: On dynamics and transport near the polar mesopause in summer, *J. Geophys. Res.*, **94**, 14617- 14628.

Nedoluha, G.E., R. M. Bevilacqua, R. M. Gomez, W. B. Waltman, B. C. Hicks, D L. Thacker, W. A. Matthews, 1996: Measurements of water vapor in the middle atmosphere and implications for mesospheric transport, *J. Geophys. Res.*, **101**, 21183-21193.

Norton, W. A. and J. Thuburn, 1996: The two-day wave in the middle atmosphere GCM, *Geophys. Res. Lett.*, **2**3, 2113-2116, 1996.

Norton, W. A. and J. Thuburn, 1997: The mesosphere in the extended UGAMP GCM, *Gravity Wave Processes and Their Parametrization in Global Climate Models*, vol. 50, K. Hamilton, ed., Springer-Verlag.

Olivero, J. J. and G. E. Thomas, 2001: Evidence for changes in greenhouse gases in the mesosphere, **28**, *Adv. Space Res.*, 931-936.

Orsolini, Y. J., V. Limpasuvan, and C. B. Leovy, 1997: The tropical stratopause in the UKMO assimilated analyses: Evidence for a 2-day wave and inertial circulations,

Quart. J. Roy. Meteor. Soc., **123***,* 1707-1724.

Palo, S. E., et. al., 1997: An intercomparison between the GSWM, UARS, and ground based radar observations: a case-study in January 1993, *Ann. Geophys.*, **15**, 1123-1141.

Pfister, L., 1985: Baroclinic instability of easterly jets with applications to the summer mesosphere, *J. Atmos. Sci.*, **42**, 313-330.

Plumb, R. A., 1983: Baroclinic instability at the Summer Mesosphere: a mechanism for the quasi-two-day wave?, *J. Atmos. Sci.*, **40**, 262-270.

Plumb, R. A. Vincent, and R. L. Craig, 1987: The quasi-two-day wave event of January 1984 and its impact on the mean mesospheric circulation, *J. Atmos. Sci.*, **44**, 3030-3036.

Polvani, L. M.,D. W. Waugh, and R. A. Plumb, 1995: On the subtropical edge of the stratospheric surf zone, *J. Atmos. Sci.*, **52**, 1288-1309.

Pumphrey, H. C. and R. S. Harwood, 1997: Water vapour and ozone in the mesosphere as measured by UARS MLS, *Geophys. Res. Lett.*, **24**, 1399-1402.

Randel, W. J., 1994: Observations of the 2-day wave in NMC stratospheric analyses, *J. Atmos. Sci.*, **51**, 306-313.

Reber, C. A., C. E. Trevathan, R. J. McNeal, and M. R. Lyther, 1993: The Upper Atmosphere Research Satellite (UARS) mission, *J. Geophys. Res.*, **98**, 10643-10647.

Salby, M. L., 1981: Rossby normal modes in nonuniform background conditions. Part II: Equinox and solstice conditions, *J. Atmos. Sci*., **38**, 1827-1840.

Salby, M. L., 1982a: Sampling theory for asynoptic satellite observations, part I: space-time spectra, resolution, and aliasing, *J. Atmos. Sci.*, **39**, 2577-2600.

Salby, M. L., 1982b: Sampling theory for asynoptic satellite observations, part II: fast Fourier synoptic mapping, *J. Atmos. Sci.*, **39**, 2601-2614.

Shepherd, M.G., W. E. Ward, B. Prawirosoehardjo, R. G. Roble, S. P. Zhang, D. Y. Wang, 1999: Planetary scale and tidal perturbations in mesospheric temperature observed by WINDII, *Earth Planets and Space*, **15**, 593-610.

Wu, D. L., O. B. Hays, W. R. Skinner, A. R. Marshall, M. D. Burrage, R. S. Lieberman, and D. A. Ortland, 1993: Observations of the quasi 2-day wave from the High Resolution Doppler Image on UARS, *Geophys. Res. Lett.*, **24**, 2853-2856.

Wu, D. L., E. F. Fishbein, W. G. Read, and J. W. Waters, 1996: Excitation and evolution of the quasi-2-day wave observed in UARS/MLS temperature measurements, *J. Atmos. Sci.*, **53**, 728-738.

Wu, D. L., W. G. Read, Z. Shippony, T. Leblanc, T. J. Duck, D. A. Ortland, R. J. Seca, P. S. Argall, J. Oberheide, A. Hauchecorne, P. Keckhut, C. Y. She, and D. A. Krueger, 2002: Mesospheric temperature from UARS MLS: retrieval and validation, *J. Atmos. Solar-Terr. Phys.*, in review.

Wu. D. L. and J. W. Waters, 1996: Gravity-wave-scale temperature fluctuations seen by the UARS MLS, *Geophys. Res. Lett.*, **23**, 3289-3292.

Wu. D. L. and J. W. Waters, 1996: Satellite observations of atmospheric variances: a possible indication of gravity waves, *Geophys. Res. Lett.*, **23**, 3631-3634.

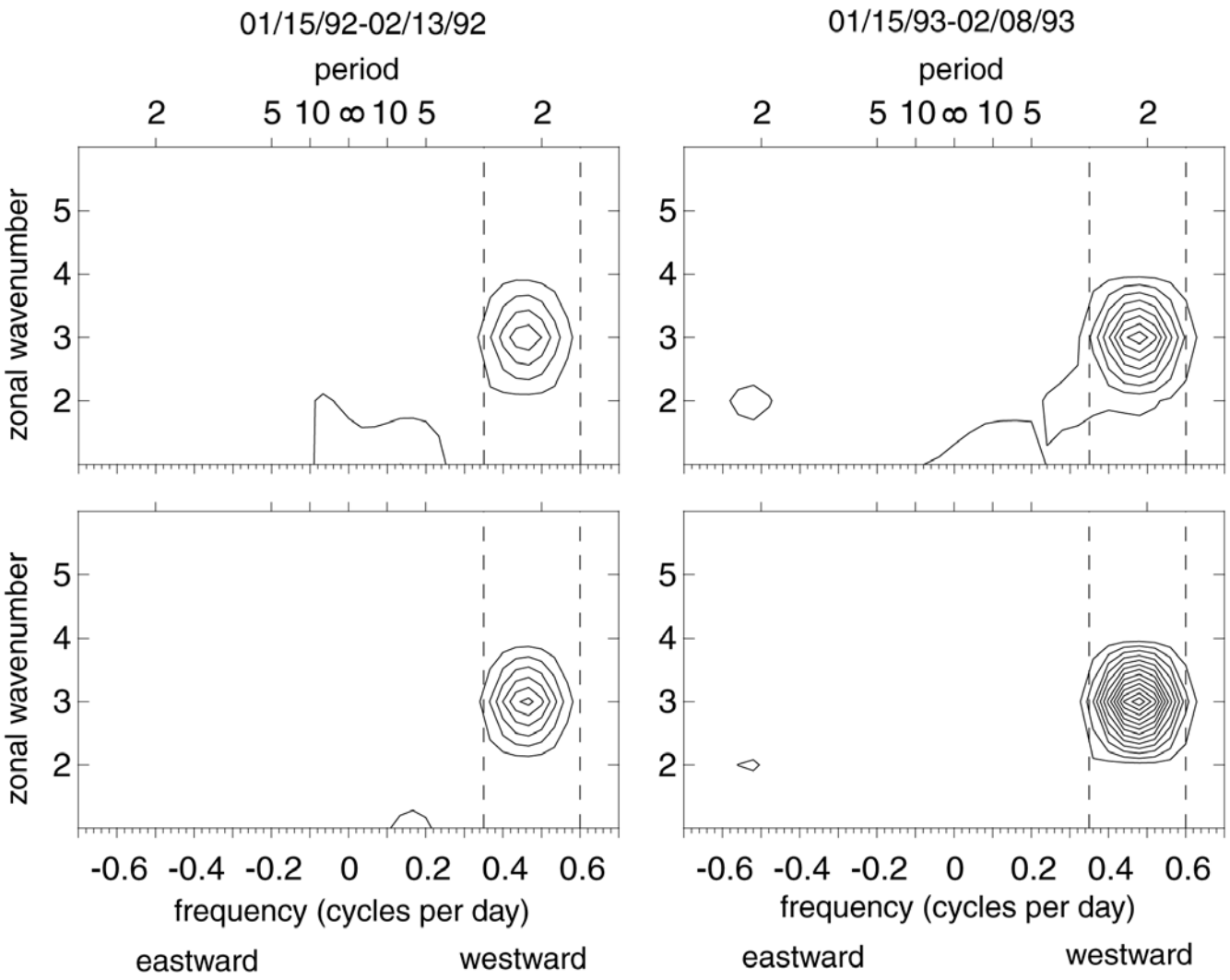

Fig. 1. Spatially averaged power spectra of water and temperature between 70°S-18°S in latitude and between 0.10 and 0.0046 hPa (approximately, 65-86 km). Water (temperature) contour interval is 0.0025 $ppmv^2$ (0.25 K^2) starting from 0.0025 $ppmv^2$ (0.25 K^2). The frequency range between 0.35 cycles per day (cpd) and 0.60 cpd (as marked by dashed lines) encompasses the two-day wave and is used for subsequent analyses.

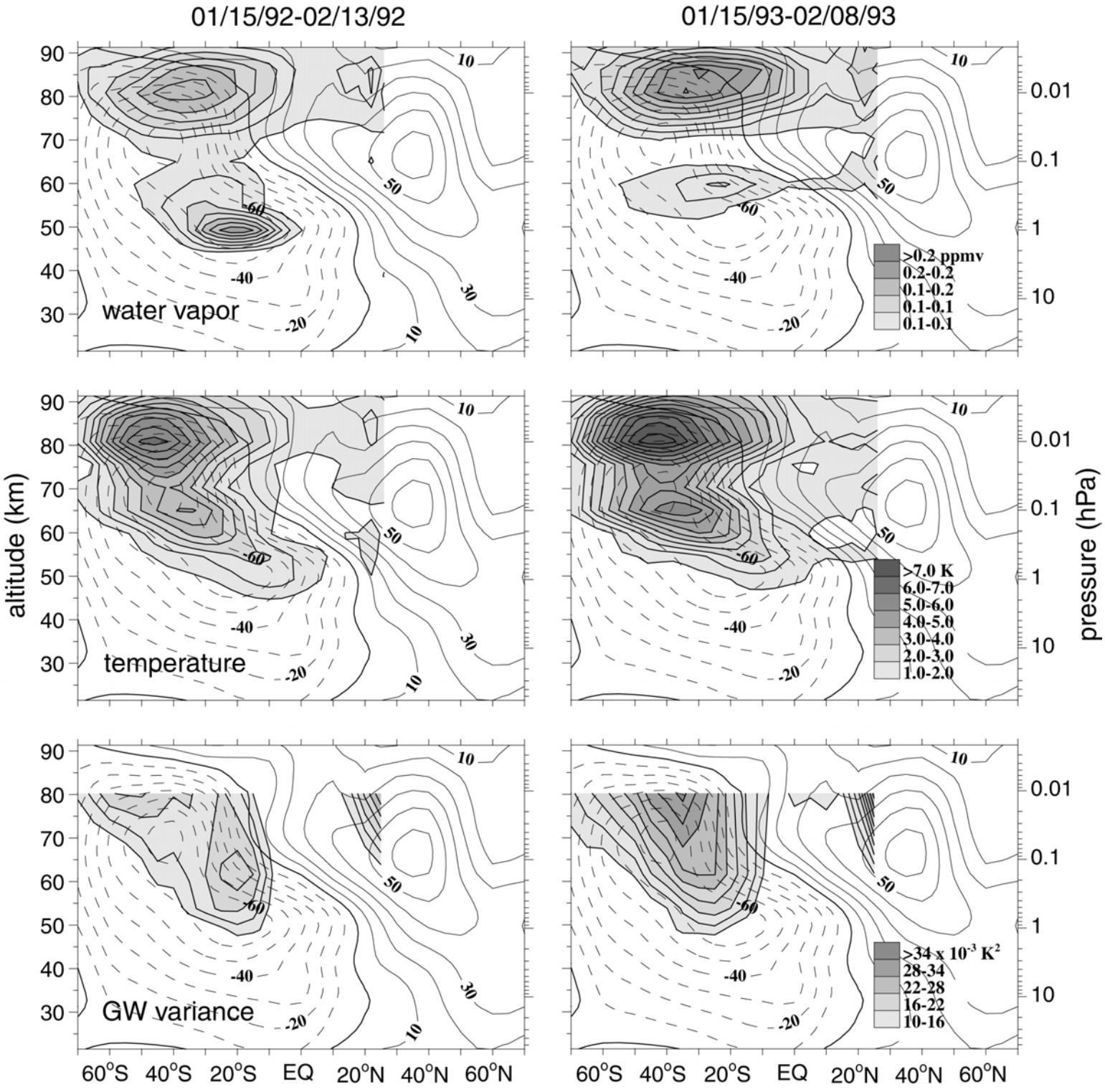

Fig. 2. Meridional cross-section of the two-day wave amplitudes. The wave amplitudes are given as filled contours. The CIRA mean zonal wind is superimposed as unfilled contours. The top (middle, bottom) row is for water vapor (temperature, gravity wave variance). The left (right) column is for analyzed period during 1992 (1993).

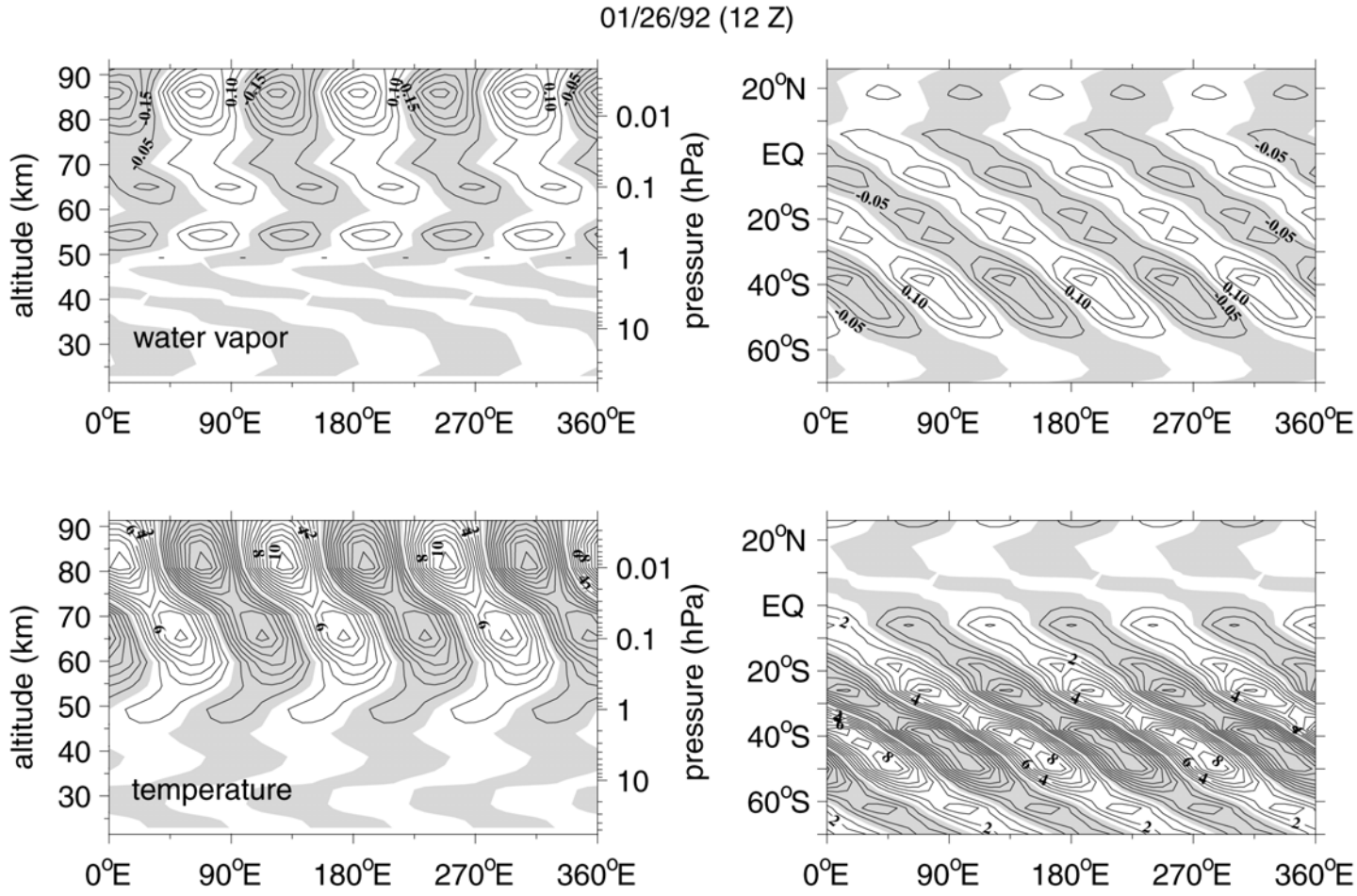

Fig. 3. The two-day wave perturbations for water (top row) and temperature (bottom row) during Jan. 26, 1992. The left column shows the longitude-height section at 38°S. The right column shows the longitude-latitude section at 0.01 hPa (~80 km). These wave structures are also observed in 1993. Negative perturbations are shaded.

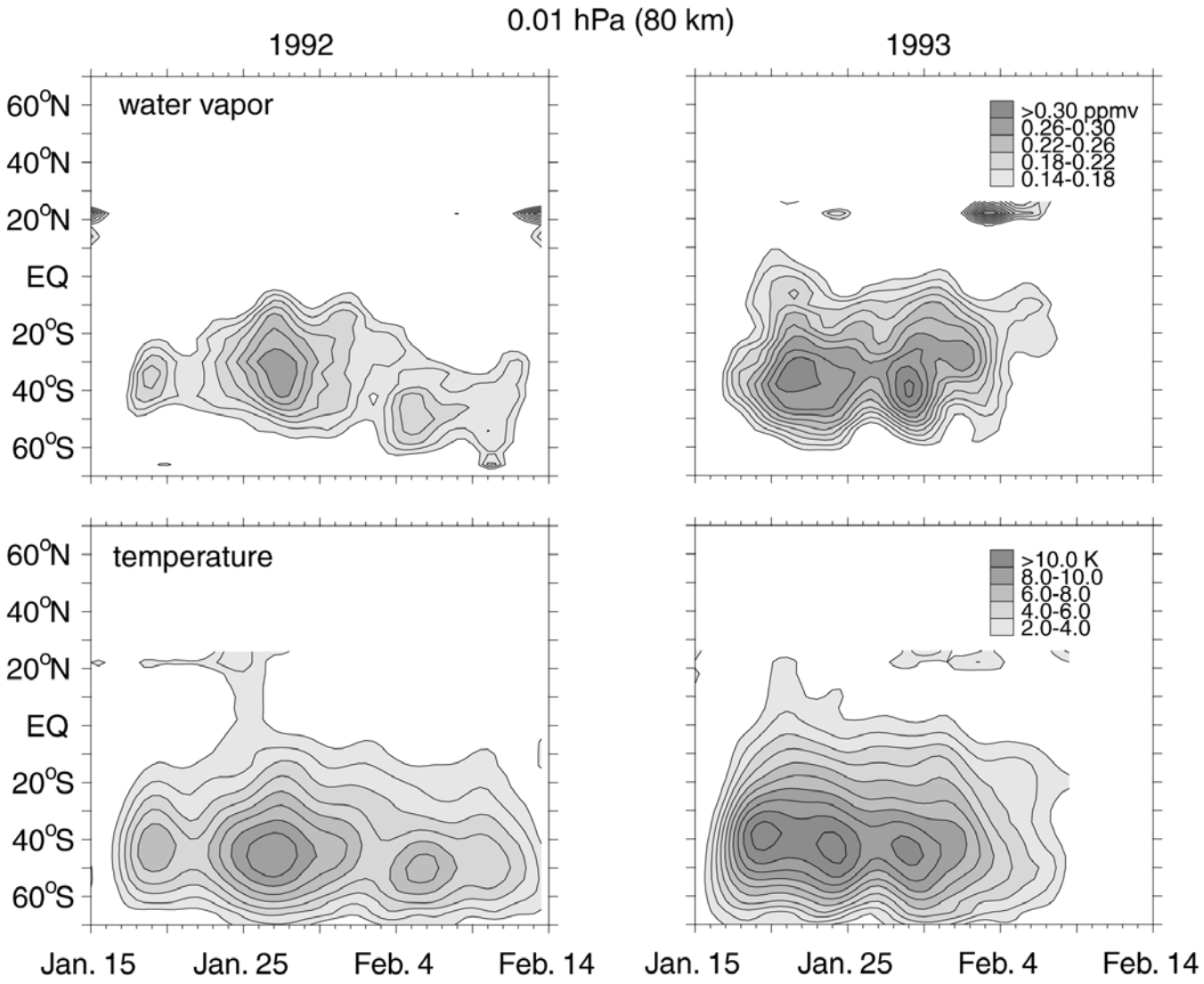

Fig. 4. Two-day wave amplitude evolution at 0.01 hPa (about 80 km). Top (bottom) row is for water vapor (temperature). Left (right) column is for year 1992 (1993).

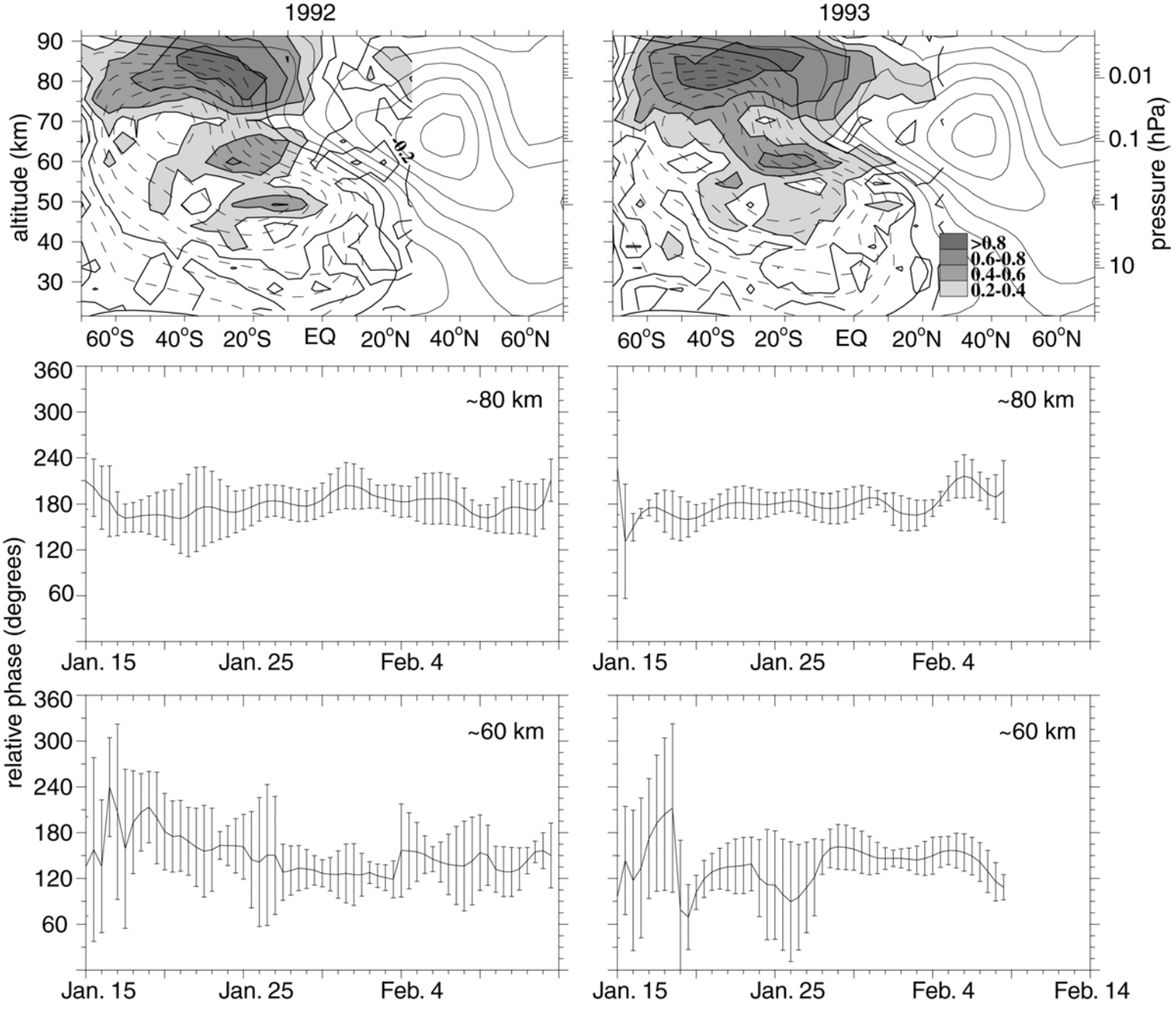

Fig. 5. (Top row) Temporal correlation values of the two-day water vapor wave amplitude and two-day temperature wave amplitude. Regions where of positive correlation values greater or equal to 0.2 are shaded. (Middle row) Latitudinal average (30^oS-46^oS) phase difference between two-day water and temperature wave at 0.01 hPa (~80 km). The phase difference is the difference in longitudinal location of the wave perturbation peak. For zonal wavenumber 3, 180^o phase difference corresponds to about 60^o longitude displacement. The error bars denote phase differences that are one standard deviation away. (Bottom row) Same as the middle row except for 0.22 hPa (~60 km)

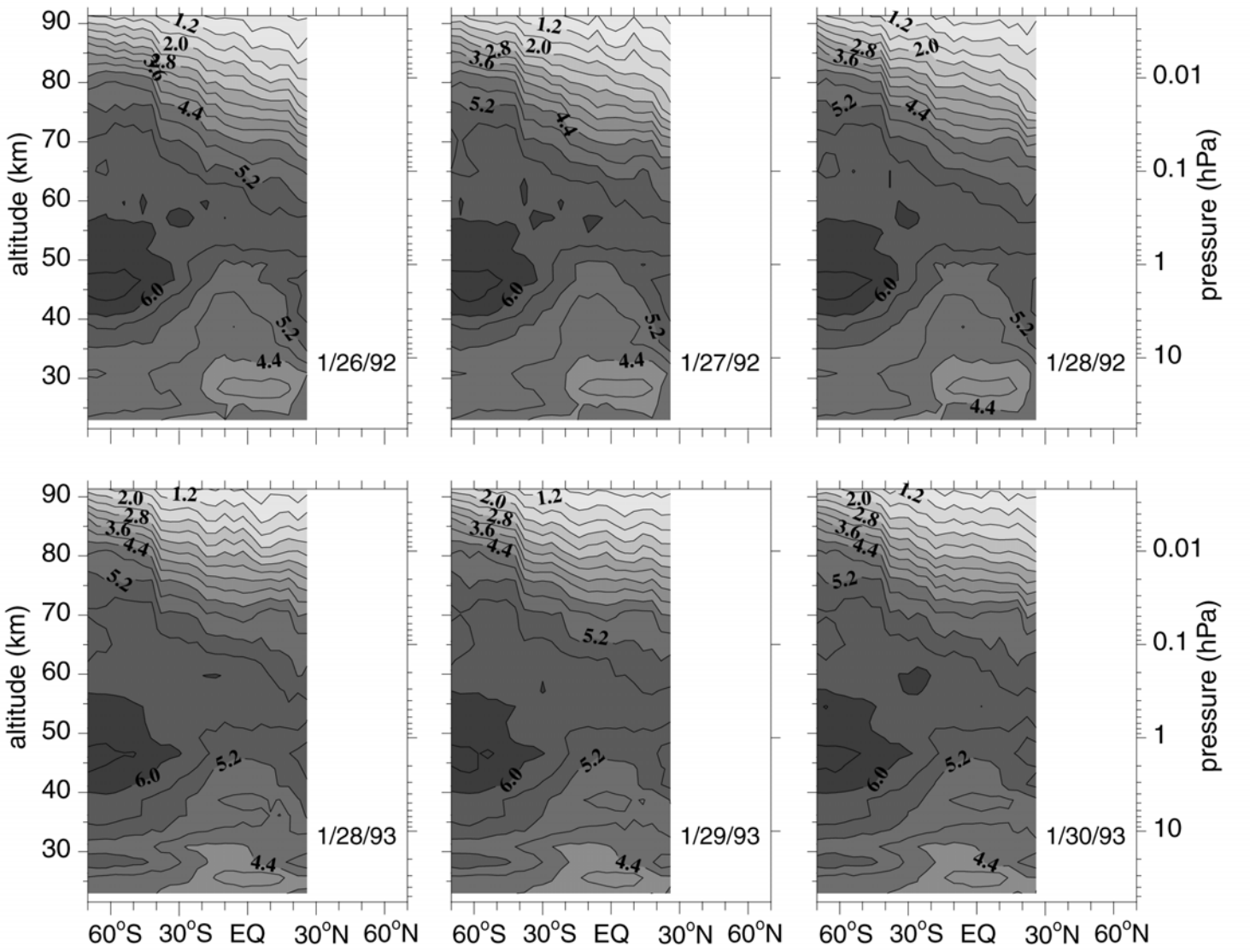

Fig. 6. Selected meridional cross-sections of zonal mean water vapor during 1992 (top) and 1993 (bottom) when the two-day wave is relatively strong. Darker shading denotes wetter air.

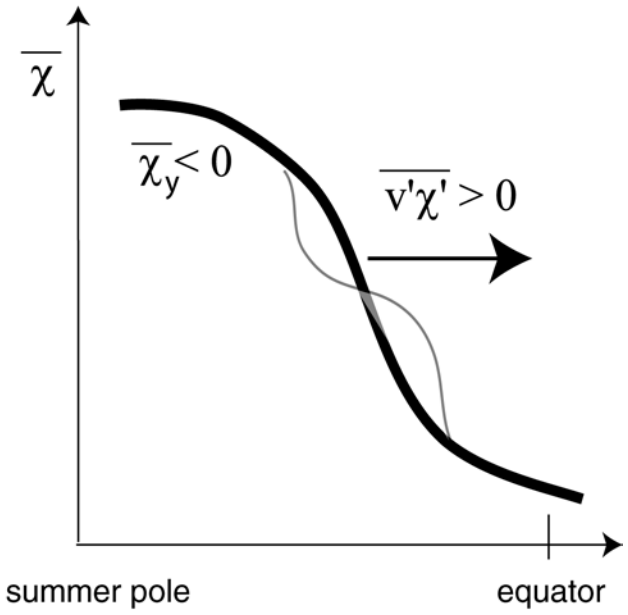

Fig. 7. A schematic of the latitudinal distribution of the zonal mean H_2O tracer (χ) during wave growth. The thick line is the background tracer distribution showing a large meridional gradient. The superimposed thin line is the perturbation as a result of the wave presence. Wave perturbations tend to flatten the meridional gradient through equatorward flux of tracer.

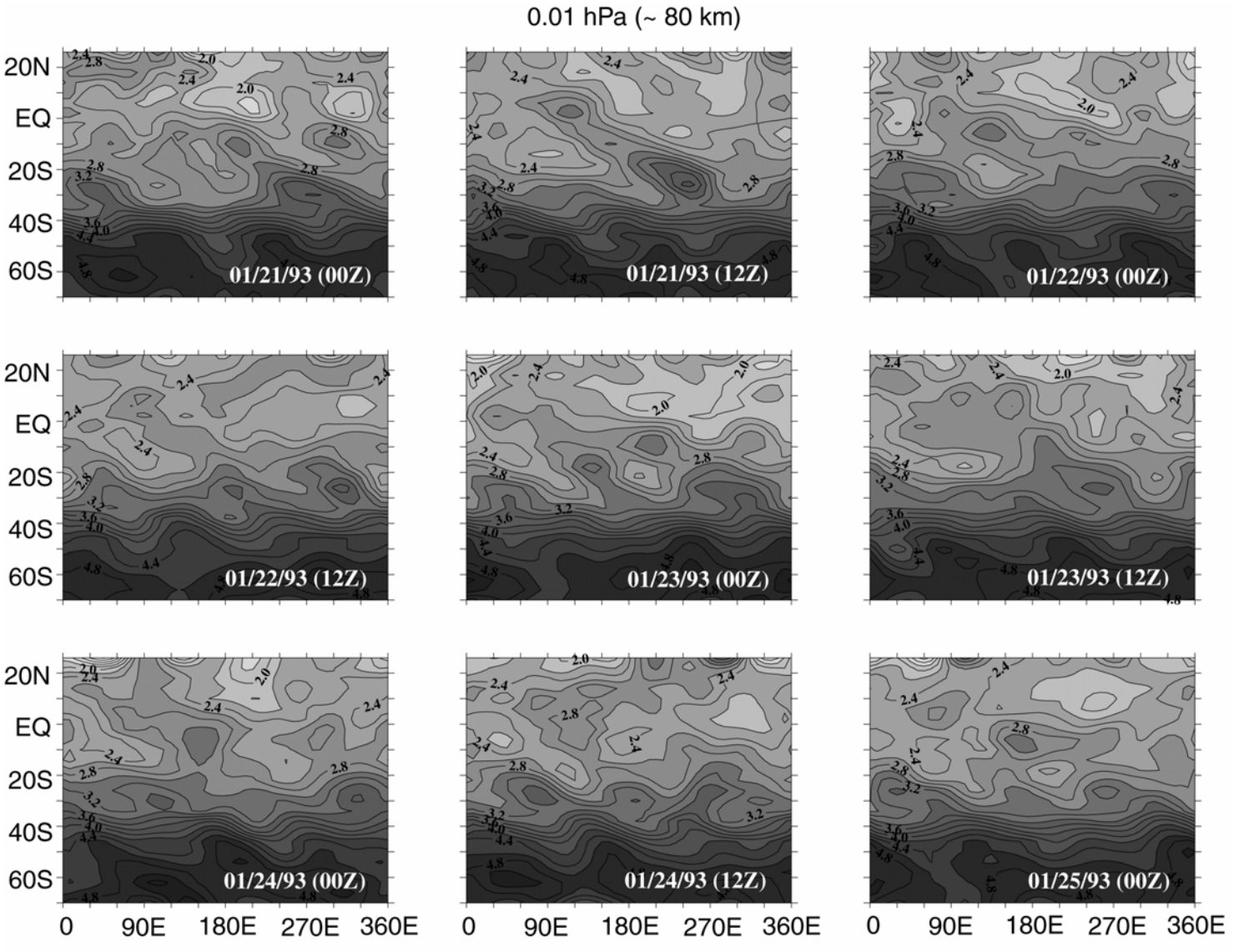

Fig. 8a. Twice-daily maps of H_2O during January 1993 at 0.01 hPa (~80 km). Darker shading denotes wetter air.

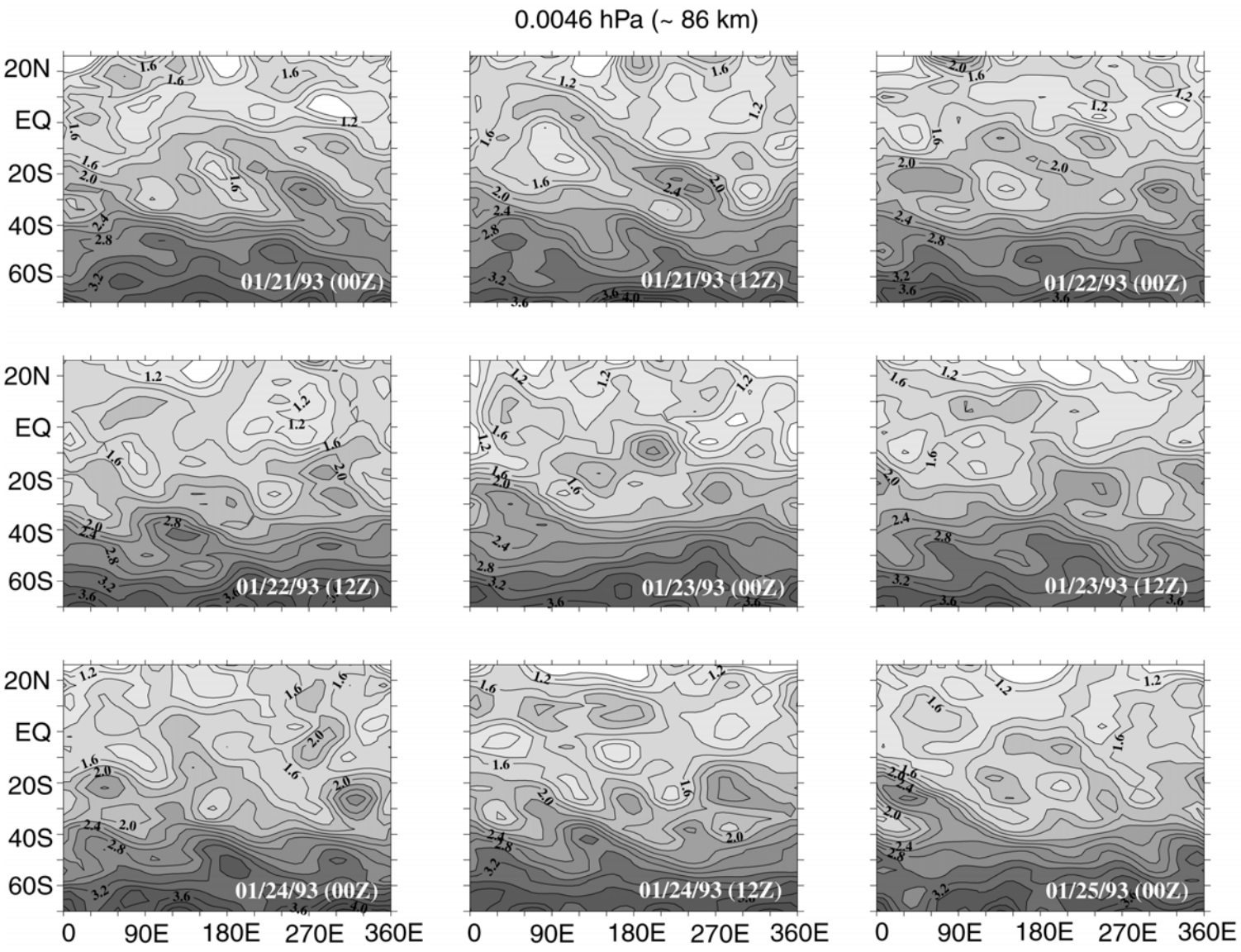

Fig. 8b. Twice-daily maps of H_2O during January 1993 at 0.0046 hPa (~86 km). Darker shading denotes wetter air